scientific reports

OPEN

Adiabatons in a double tripod coherent atom-light coupling scheme

Viačeslav Kudriašov[1], Hamid R. Hamedi[1]✉ & Julius Ruseckas[2]

Optical adiabatons are specific shape-invariant pulse pairs propagating at the reduced group velocity and without optical absorption in the medium. The purpose of this study is to analyze the possibility of adiabaton formation in multilevel atomic systems with the focus on M-type and double tripod (DT) systems having five energy levels and different interaction configurations. Findings show that the M-type atomic system is prone to intensity dependent group velocity and pulse front steepening which prevents the formation of long range optical adiabatons. In contrast, the DT atomic system is quite favorable for the formation of optical adiabatons exhibiting two different optical field configurations propagating with invariant shape.

Keywords Multilevel atomic systems, Electromagnetically induced transparency, Nonlinear propagation, Adiabatic approximation, Adiabatons

Precise control of light-matter interactions is crucial in optics research and applications. Remarkable progress in this field has been made using quantum interference in resonant media[1–3], where materials can be manipulated into specific quantum states to enhance or suppress light absorption. One notable technique that exemplifies this approach is electromagnetically induced transparency (EIT)[2,4–6], allowing a material to become transparent to a specific light frequency that it would normally absorb. Beyond the transparency, EIT can also lead to a wealth of other fascinating effects. These include the formation of non-absorbing dark states[7], slow group velocities (slow light)[8], giant nonlinearities[9–12] and other phenomena[13–29]. This underscores the power of quantum interference in achieving precise control over the optical response making EIT-related research an active area until present[30–32]. Notably, most of the aforementioned effects can be observed in simple three- or four-level atomic media driven by several coherent laser fields (usually probe and pump) tuned to the resonant atomic transitions. However, the possibilities of coherent control substantially increase for the light-atom configurations with larger number of atomic levels. For these type of multilevel systems more sophisticated interaction effects and richer dynamics can be observed. Recent studies show that EIT paradigm can been extended further into the nonlinear regime, where EIT-enhanced nonlinearities support shape-preserving optical pulses beyond the weak-probe limit[33–35].

Typically, EIT-based research focuses on conditions where the probe field is much weaker than the coupling field. However, in practical applications, such as achieving extremely low group velocities, the intensity of the coupling laser field must be kept quite low as well. This requirement presents a challenge for ultra-slow light propagation because the probe field needs to be significantly weak to maintain the validity of the weak probe approximation. On the other hand, in order to be detectable, the probe field should also be strong enough, so that the weak probe approximation is often not met. This issue has led to an interest in studying the effects of stronger probe fields in EIT scenarios. Grobe et al.[36] addressed this by finding an exact solution to the coupled nonlinear Maxwell-Schrödinger equations for the Λ scheme under so-called adiabatic conditions. The solution permits the waves of arbitrary shapes to propagate, retaining their shapes relatively unchanged after some initial reshaping. These shape-preserving waves are known as adiabatons.

An optical adiabaton is a set of shape-invariant pulses with slowly changing envelopes that propagate at reduced group velocities without optical absorption in the medium. Adiabatons represent a nonlinear pulse propagation regime under EIT conditions, where the intensity of the probe field is comparable to that of the control field, allowing the adiabatic approximation to hold[37]. Briefly, the adiabatic approximation means that the optical fields have large intensities and change slowly, so that the excited states are not populated. On the contrary, when the system deviates from the adiabaticity, the pulses experience absorption, attenuation, reshaping, and steepening effects. As such, the adiabatons are of significant interest in the field of coherent

[1]Institute of Theoretical Physics and Astronomy, Vilnius University, Saulėtekio 3, LT-10257 Vilnius, Lithuania. [2]Baltic Institute of Advanced Technology, Pilies St. 16-8, LT-01403 Vilnius, Lithuania. ✉email: hamid.hamedi@tfai.vu.lt

control and quantum optics, having applications in quantum information processing, precision spectroscopy, and optical communication, where the control over group velocity and pulse shape is crucial.

The theoretical prediction of adiabatons in a Λ system[36] was soon experimentally confirmed[38]. Subsequent studies on adiabatons explored this phenomenon in various systems and conditions[39–44]. For instance, a four-level double-Λ scheme was used to demonstrate the pulse matching and adiabaton-type propagation[39]. Temporal reshaping and compression of a probe pulse, due to its group velocity's dependence on the control field, were also studied[40,41]. Two types of adiabatons with zero and non-zero energy in Λ and ladder schemes, respectively, were analyzed[42]. Additionally, two pairs of adiabatically propagating pulses at different group speeds — fast and slow adiabatons — were found in a tripod system[43]. Adiabatons for five-level systems have only been analyzed in a simple five-level double-Λ scheme[44].

In multilevel atomic systems, as was already mentioned, the increased number of energy levels and interacting laser fields provides enhanced control over the formation and dynamics of shape-preserving optical pulses. However, the conditions under which adiabatic pulse propagation — specifically, the formation of optical adiabatons — can occur have not been fully investigated in complex EIT-based schemes. In this work, we address this open question by theoretically analyzing adiabatic pulse propagation in two well-known multilevel atomic systems: the M-type[45,46] and the double tripod (DT) configurations[47–51]. Both schemes feature five distinct energy levels, but differ in field arrangements: the M-type system involves four laser fields in an M-shaped configuration, whereas the DT setup includes six fields forming a pair of interconnected tripods (Fig. 1).

Importantly, the DT scheme exhibits several remarkable properties not present in simpler systems, like Λ or M. In particular, DT setup supports two probe beams at different frequencies which couple together via four control fields and atomic coherences. This arrangement leads to the formation of a two-component (spinor) slow light with distinct characteristics[47,51]. In such a medium, only specific combinations of the probe fields (normal modes) can propagate through the atomic cloud with well-defined and differing group velocities. As current study demonstrates, under suitable conditions in DT system the six optical fields after some propagation distance form two distinct combinations that propagate with a stable, shape-preserving structure. Those combinations of optical fields represent adiabatons. On the contrary, the M-type system suffers from an intensity-dependent group velocity that causes pulse front steepening and ultimately a breakdown of adiabaticity conditions. These findings highlight a key aspect of our work: adiabaton formation is not universally supported across all EIT-enabled multilevel systems, even when they share similar energy-level structures. Rather, the possibility of stable, shape-preserving propagation is critically dependent on the specific interaction topology and coupling geometry.

The paper is structured as follows. In Sec. 1 we examine light pulse propagation in a multilevel M-type system, which is not favorable to adiabaton formation. Then, in Sec. 2 we present calculations and analyze adiabaton propagation in a DT system. Finally, we conclude with a discussion and summarize our findings in Sec. 3. Additionally, for illustration of the approach used in the paper, in Supplementary Information we present some well-established analytical results for a simple three level Λ system and two optical fields, as previously described in Refs.[36,37].

Propagation of light pulses in M-type system

Equations of motion for atoms and fields

We consider a M-type atomic system (Fig. 1a) involving three metastable ground states $|0\rangle$, $|1\rangle$ and $|2\rangle$, as well as two excited states $|e_1\rangle$ and $|e_2\rangle$. Four laser fields with the Rabi frequencies $\Omega_{j,l}$ induce resonant transitions $|l\rangle \rightarrow |e_j\rangle$; here the $j = 1, 2$ and $l = 0, j$. Applying the rotating wave approximation (RWA), the atomic Hamiltonian in the rotating frame with respect to the atomic levels reads

$$H_{\mathrm{M}} = \sum_{j=1}^{2} \left\{ -\frac{1}{2} \left(\Omega_{j,0} |e_j\rangle\langle 0| + \Omega_{j,j} |e_j\rangle\langle j| + \mathrm{H.c.} \right) - \frac{i}{2} \Gamma |e_j\rangle\langle e_j| + \delta_j |j\rangle\langle j| \right\}, \tag{1}$$

where δ_j are two-photon detunings. The losses in the Hamiltonian (1) are taken into account in an effective way by introducing a rate Γ of the excited state decay. In order to simplify the mathematical description of the system while keeping the relevant physical details, we characterize the state of an atom using a state vector

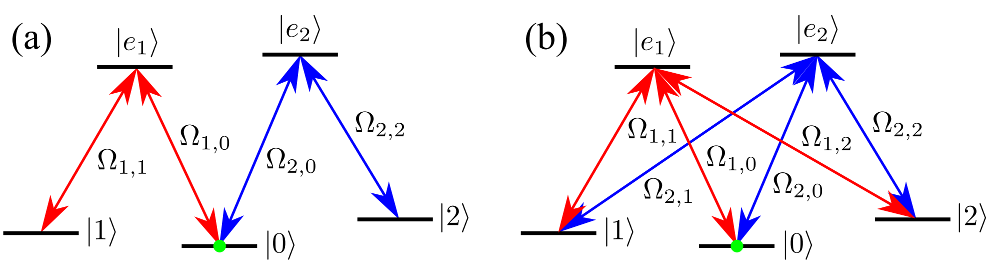

Fig. 1. (**a**) Five level M-type atomic system. Four laser beams with the Rabi frequencies $\Omega_{1,0}$, $\Omega_{1,1}$, $\Omega_{2,2}$ and $\Omega_{2,0}$ act on atoms characterized by three hyperfine ground levels $|0\rangle$, $|1\rangle$ and $|2\rangle$ and two excited levels $|e_1\rangle$ and $|e_2\rangle$; (**b**) Five level DT atomic system. Six laser beams with the Rabi frequencies $\Omega_{1,0}$, $\Omega_{1,1}$, $\Omega_{1,2}$ and $\Omega_{2,0}$, $\Omega_{2,1}$, $\Omega_{2,2}$ act on atoms characterized by three hyperfine ground levels $|0\rangle$, $|1\rangle$ and $|2\rangle$ and two excited levels $|e_1\rangle$ and $|e_2\rangle$. Both systems initially reside in the ground level $|0\rangle$ as marked by green circles.

$|\Psi\rangle = \sum_{l=0}^{2} \psi_l |l\rangle + \sum_{j=1}^{2} \psi_{e_j} |e_j\rangle$, as in Refs.[36,52], instead of a more complete description that involves a density matrix[37,53]. The time-dependent Schrödinger equation $i\hbar\partial_t|\Psi\rangle = H_{\mathrm{M}}|\Psi\rangle$ for the atomic state-vector $|\Psi\rangle$ yields the following equations for the atomic probability amplitudes ψ_l, ψ_{e_j}:

$$i\partial_t\psi_0 = -\frac{1}{2}\Omega^*_{1,0}\psi_{e_1} - \frac{1}{2}\Omega^*_{2,0}\psi_{e_2}\,, \tag{2}$$

$$i\partial_t\psi_1 = \delta_1\psi_1 - \frac{1}{2}\Omega^*_{1,1}\psi_{e_1}\,, \tag{3}$$

$$i\partial_t\psi_2 = \delta_2\psi_2 - \frac{1}{2}\Omega^*_{2,2}\psi_{e_2}\,, \tag{4}$$

$$i\partial_t\psi_{e_1} = -\frac{i}{2}\Gamma\psi_{e_1} - \frac{1}{2}\Omega_{1,0}\psi_0 - \frac{1}{2}\Omega_{1,1}\psi_1\,, \tag{5}$$

$$i\partial_t\psi_{e_2} = -\frac{i}{2}\Gamma\psi_{e_2} - \frac{1}{2}\Omega_{2,0}\psi_0 - \frac{1}{2}\Omega_{2,2}\psi_2\,. \tag{6}$$

On the other hand, the Rabi frequencies of the laser fields obey the following propagation equations

$$(\partial_t + c\partial_z)\Omega_{1,0} = \frac{i}{2}g\psi_{e_1}\psi_0^*\,, \tag{7}$$

$$(\partial_t + c\partial_z)\Omega_{2,0} = \frac{i}{2}g\psi_{e_2}\psi_0^*\,, \tag{8}$$

$$(\partial_t + c\partial_z)\Omega_{1,1} = \frac{i}{2}g\psi_{e_1}\psi_1^*\,, \tag{9}$$

$$(\partial_t + c\partial_z)\Omega_{2,2} = \frac{i}{2}g\psi_{e_2}\psi_2^*\,, \tag{10}$$

where the parameter g characterizes the strength of coupling of the light fields with the atoms. For simplicity here we have assumed that the coupling strength g is the same for both laser fields. The coupling strength g is related to the optical depth α as $g = c\Gamma\alpha/L$, where L is the length of the medium.

Coupled and uncoupled states

For simplifying of analysis it is convenient to introduce coupled $|\mathrm{C}\rangle$ and uncoupled $|\mathrm{U}\rangle$ atomic states. Coupled states are superpositions of the ground states that are directly connected to the excited states via optical fields, whereas uncoupled states are not coupled to the excited states. Let us define two unnormalized and non-orthogonal to each other coupled states as $|\mathrm{C}_j\rangle = \chi_j^*|0\rangle + |j\rangle$ where $\chi_j = \Omega_{j,0}/\Omega_{j,j}(\,j = 1,2)$. Then, a normalized uncoupled state (orthogonal to both coupled states) can be defined as $|\mathrm{U}\rangle = \frac{1}{N_0}(|0\rangle - \chi_1|1\rangle - \chi_2|2\rangle)$ where $N_0 = \sqrt{1 + |\chi_1|^2 + |\chi_2|^2}$ is a normalization factor. Following this notation the amplitudes to find an atom in the coupled and uncoupled states read

$$\psi_{\mathrm{C}_j} = \langle \mathrm{C}_j|\Psi\rangle = \chi_j\psi_0 + \psi_j\,, \tag{11}$$

$$\psi_{\mathrm{U}} = \langle \mathrm{U}|\Psi\rangle = \frac{1}{N_0}(\psi_0 - \chi_1^*\psi_1 - \chi_2^*\psi_2)\,. \tag{12}$$

The initial atomic amplitudes then can be expressed as

$$\psi_0 = \frac{1}{N_0}\left(\psi_{\mathrm{U}} + \frac{1}{N_0}\chi_1^*\psi_{\mathrm{C}_1} + \frac{1}{N_0}\chi_2^*\psi_{\mathrm{C}_2}\right)\,, \tag{13}$$

$$\psi_1 = \psi_{\mathrm{C}_1} - \chi_1\psi_0 = -\frac{\chi_1}{N_0}\psi_{\mathrm{U}} + \cdots\,, \tag{14}$$

$$\psi_2 = \psi_{\mathrm{C}_2} - \chi_2\psi_0 = -\frac{\chi_2}{N_0}\psi_{\mathrm{U}} + \cdots\,. \tag{15}$$

Using the coupled states the system Hamiltonian (1) can be rewritten as

$$H_{\mathrm{M}} = \sum_{j=1}^{2}\left\{-\frac{1}{2}\left(\Omega_{j,j}|e_j\rangle\langle \mathrm{C}_j| + \Omega^*_{j,j}|\mathrm{C}_j\rangle\langle e_j|\right) + \delta_j|j\rangle\langle j| - \frac{i}{2}\Gamma|e_j\rangle\langle e_j|\right\}, \tag{16}$$

The equations for the atomic amplitudes in terms of coupled and uncoupled states take the form

$$i\partial_t\psi_{\mathrm{U}} = \Delta\psi_{\mathrm{U}} + \cdots\,, \tag{17}$$

$$i\partial_t\psi_{C_1} = V_1\psi_U - \frac{1}{2}\Omega^*_{1,1}N_1^2\psi_{e_1} - \frac{1}{2}\Omega^*_{2,0}\chi_1\psi_{e_2} + \cdots\,, \tag{18}$$

$$i\partial_t\psi_{C_2} = V_2\psi_U - \frac{1}{2}\Omega^*_{1,0}\chi_2\psi_{e_1} - \frac{1}{2}\Omega^*_{2,2}N_2^2\psi_{e_2} + \cdots\,, \tag{19}$$

$$i\partial_t\psi_{e_1} = -\frac{i}{2}\Gamma\psi_{e_1} - \frac{1}{2}\Omega_{1,1}\psi_{C_1}\,, \tag{20}$$

$$i\partial_t\psi_{e_2} = -\frac{i}{2}\Gamma\psi_{e_2} - \frac{1}{2}\Omega_{2,2}\psi_{C_2}\,. \tag{21}$$

Here, $V_1 = \frac{1}{N_0}(i\partial_t - \delta_1)\chi_1, V_2 = \frac{1}{N_0}(i\partial_t - \delta_2)\chi_2$ represent the non-adiabatic coupling coefficients,

$$\Delta = \frac{1}{N_0}i\partial_t\frac{1}{N_0} + \frac{\chi_1}{N_0}i\partial_t\frac{\chi_1^*}{N_0} + \frac{\chi_2}{N_0}i\partial_t\frac{\chi_2^*}{N_0} + \delta_1\frac{|\chi_1|^2}{N_0^2} + \delta_2\frac{|\chi_2|^2}{N_0^2} \tag{22}$$

denotes the detuning, and $N_1 = \sqrt{1+|\chi_1|^2}$, $N_2 = \sqrt{1+|\chi_2|^2}$ are the normalization factors for the unnormalized coupled states. Note, that terms containing amplitudes ψ_{C_1}, ψ_{C_2} were omitted in the Eqs. (14)-(15), (17)-(19) being not relevant for the first order of the adiabatic approximation.

Adiabatic approximation

The term "adiabatic" means that the rate of change of the varying quantities is sufficiently small, so that a system remains in a quasi-steady state. Here, for the atom-light system adiabatic approximation implies that the optical fields have large intensities and change slowly, so that the excited states are not populated. Violation of the conditions for the adiabatic approximation leads to the increase of population of the excited states and corresponding losses due to their decay.

Let us consider a situation where the light fields are slowly changing and have large intensities. In this situation we can apply the adiabatic approximation. Neglecting small amplitudes of the coupled states ψ_{C_1} and ψ_{C_2} in Eqs. (18), (19) leads to a following pair of equations

$$2V_1\psi_U = \Omega^*_{1,1}N_1^2\psi_{e_1} + \Omega^*_{2,0}\chi_1\psi_{e_2}\,, \tag{23}$$

$$2V_2\psi_U = \Omega^*_{1,0}\chi_2\psi_{e_1} + \Omega^*_{2,2}N_2^2\psi_{e_2}, \tag{24}$$

with the solution

$$\psi_{e_1} = 2W_1\psi_U\,, \tag{25}$$

$$\psi_{e_2} = 2W_2\psi_U\,, \tag{26}$$

where

$$W_1 = \frac{1}{\Omega^*_{1,1}N_0^2}(N_2^2V_1 - \chi_1\chi_2^*V_2) = \frac{1}{\Omega^*_{1,1}N_0^3}[N_2^2(i\partial_t - \delta_1)\chi_1 - \chi_1\chi_2^*(i\partial_t - \delta_2)\chi_2]\,, \tag{27}$$

$$W_2 = \frac{1}{\Omega^*_{2,2}N_0^2}(N_1^2V_2 - \chi_2\chi_1^*V_1) = \frac{1}{\Omega^*_{2,2}N_0^3}[N_1^2(i\partial_t - \delta_1)\chi_2 - \chi_2\chi_1^*(i\partial_t - \delta_2)\chi_1]\,. \tag{28}$$

On the other hand, Eqs. (20), (21) relate ψ_{C_1}, ψ_{C_2} to ψ_{e_1}, ψ_{e_2} as $\psi_{C_1} = -i(\Gamma/\Omega_{1,1})\psi_{e_1}$ and $\psi_{C_2} = -i(\Gamma/\Omega_{2,2})\psi_{e_2}$. Neglecting the decay of adiabatons, Eq. (17) for the amplitude of the uncoupled state becomes $i\partial_t\psi_U = \Delta\psi_U$. Inserting Eqs. (25), (26) into Eqs. (7)–(10) we get

$$(\partial_t + c\partial_z)\Omega_{1,0} = i\frac{g}{N_0}W_1\,, \tag{29}$$

$$(\partial_t + c\partial_z)\Omega_{2,0} = i\frac{g}{N_0}W_2\,, \tag{30}$$

$$(\partial_t + c\partial_z)\Omega_{1,1} = -i\frac{g}{N_0}\chi_1^*W_1\,, \tag{31}$$

$$(\partial_t + c\partial_z)\Omega_{2,2} = -i\frac{g}{N_0}\chi_2^*W_2\,. \tag{32}$$

Equations (29)–(32) describe adiabatic propagation of the fields.

Matrix form of equations

From Eqs. (29)-(32) we obtain that the total Rabi frequencies $\Omega_1 = \sqrt{|\Omega_{1,1}|^2 + |\Omega_{1,0}|^2} = |\Omega_{1,1}|N_1$ and $\Omega_2 = \sqrt{|\Omega_{2,2}|^2 + |\Omega_{2,0}|^2} = |\Omega_{2,2}|N_2$ obey the equations $(\partial_t + c\partial_z)\Omega_1 = 0$ and $(\partial_t + c\partial_z)\Omega_2 = 0$, respectively. Combining Eqs. (29)-(32) we get the equations for the ratios χ_1 and χ_2

$$(\partial_t + c\partial_z)\chi_1 = ig\frac{N_1^2}{N_0}\frac{W_1}{\Omega_{1,1}}\,, \tag{33}$$

$$(\partial_t + c\partial_z)\chi_2 = ig\frac{N_2^2}{N_0}\frac{W_2}{\Omega_{2,2}}. \tag{34}$$

Introducing the two-component spinor $\chi = (\chi_1, \chi_2)^\intercal$ and using Eqs. (27), (28), (33), (34) can be written in the following matrix form

$$(c^{-1} + \hat{v}^{-1})\partial_t\chi + \partial_z\chi + i\hat{v}^{-1}\hat{\delta}\chi = 0, \tag{35}$$

where

$$\hat{v}^{-1} = \frac{g}{cN_0^4}\begin{pmatrix} \frac{N_1^2 N_2^2}{|\Omega_{1,1}|^2} & -\frac{N_1^2\chi_1\chi_2^*}{|\Omega_{1,1}|^2} \\ -\frac{N_2^2\chi_2\chi_1^*}{|\Omega_{2,2}|^2} & \frac{N_2^2 N_1^2}{|\Omega_{2,2}|^2} \end{pmatrix} = \frac{g}{c}\begin{pmatrix} \frac{1}{\Omega_1^2}\frac{N_1^4}{N_0^4} & 0 \\ 0 & \frac{1}{\Omega_2^2}\frac{N_2^4}{N_0^4} \end{pmatrix}(N_0^2 I - \chi\chi^\dagger), \tag{36}$$

is the matrix of inverse group velocity, and

$$\hat{\delta} = \begin{pmatrix} \delta_1 & 0 \\ 0 & \delta_2 \end{pmatrix}, \tag{37}$$

is the matrix of two-photon detunings.

Equal fields

Let us now consider a particular case where $\Omega_{2,0} = \Omega_{1,0}$ and $\Omega_{2,2} = \Omega_{1,1}$ at the beginning of the medium ($z = 0$). We also assume that $\delta_2 = \delta_1$. In this situation $\chi_2 = \chi_1$ at all times and positions. Equation for the propagation becomes

$$\left(c^{-1} + \frac{g}{c\Omega_1^2}\frac{N_1^4}{N_0^4}\right)\partial_t\chi_1 + \partial_z\chi_1 + i\frac{g}{c\Omega_1^2}\frac{N_1^4}{N_0^4}\delta_1\chi_1 = 0. \tag{38}$$

This equation has a similar form to the equation for the propagation of the probe field in the EIT configuration, and is also similar to the equation for Λ-type system. The group velocity is

$$v_g = \frac{c\Omega_1^2}{g}\frac{N_0^4}{N_1^4}. \tag{39}$$

Equation (39) shows that the group velocity v_g, like the group velocity of slow light, increases with the Rabi frequency Ω_1 and is inversely proportional to atom-light coupling strength *g*. In addition, the presence of the second pair of beams increases the group velocity of the adiabaton propagation because $N_0 > N_1$. Thus, parts of the pulse with larger amplitude propagate faster, which leads to changing shape of the pulse and to an instability of its wavefront.

We conducted numerical study of the equations (29)–(32) using the Gaussian input fields. The first field at the input of the atomic media is of the form $\Omega_{1,0}(0,t) = A\exp[-(t-t_0)^2/\tau_0^2]$, where $\tau_0 = 5\Gamma^{-1}$, $t_0 = 23\Gamma^{-1}$, $A = \Gamma$, while the second one is a constant $\Omega_{1,1}(0,t) = 1.5\Gamma$. Results of the calculation are shown in Fig. 2 which demonstrates significant pulse deformation and strong steepening effect at the propagation distances exceeding $25L_{\mathrm{abs}}$. Here $L_{\mathrm{abs}} = L/\alpha$ denote the resonant absorption length, and α is the optical density of the medium. This kind of pulse shape's deformation observed in M-type system has similar origin as a self-steepening effect in classical nonlinear optics[54]. The latter develops as a result of nonlinear dependence of the refractive index on pulse intensity that leads to the intensity-dependent group velocity. Commonly this effect is observed for the propagation of short laser pulses producing sharp steepening of the trailing edge of the pulse (optical shock) and accompanying spectral broadening. The effect of self-steepening is well known and the accompanying pulse behavior has been extensively studied earlier[55].

Adiabatons in double tripod system

Initial equations

Now, we investigate a DT type atomic system (Fig. 1b) involving three metastable ground states $|0\rangle$, $|1\rangle$ and $|2\rangle$, as well as excited states $|e_1\rangle$ and $|e_2\rangle$. Six laser fields with the Rabi frequencies $\Omega_{j,l}$ induce resonant transitions $|l\rangle \to |e_j\rangle$. Applying the rotating wave approximation (RWA), the atomic Hamiltonian in the rotating frame with respect to the atomic levels reads

$$H_{\mathrm{DT}} = \sum_{j=1}^{2}\left\{-\frac{1}{2}\left(\sum_{l=0}^{2}\Omega_{j,l}|e_j\rangle\langle l| + \text{H.c.}\right) + \delta_j|j\rangle\langle j| - \frac{i}{2}\Gamma|e_j\rangle\langle e_j|\right\}, \tag{40}$$

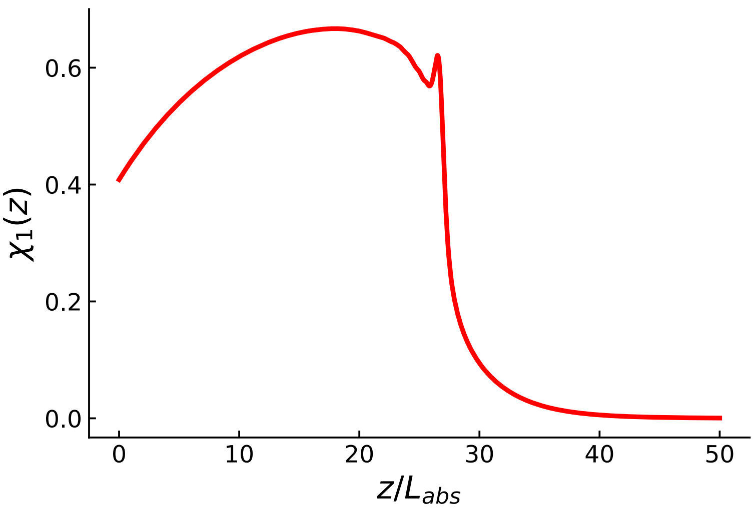

Fig. 2. Dependence of pulse amplitude ratio χ_1 on the propagation distance in M-type system calculated at time instance of $t = 26.5\Gamma^{-1}$.

where δ_j are two-photon detunings. The losses in the Hamiltonian (40) are taken into account in an effective way by introducing a rate Γ of the excited state decay. The time-dependent Schrödinger equation $i\hbar\partial_t|\Psi\rangle = H_{\mathrm{DT}}|\Psi\rangle$ for the atomic state-vector $|\Psi\rangle = \sum_{l=0}^{2}\psi_l|l\rangle + \sum_{j=1}^{2}\psi_{e_j}|e_j\rangle$ yields the following equations for the atomic probability amplitudes ψ_l, ψ_{e_j}

$$i\partial_t\psi_l = \delta_l\psi_l - \frac{1}{2}\sum_j \Omega_{j,l}^*\psi_{e_j}\,, \tag{41}$$

$$i\partial_t\psi_{e_j} = -\frac{i}{2}\Gamma\psi_{e_j} - \frac{1}{2}\sum_l \Omega_{j,l}\psi_l\,. \tag{42}$$

Here, to make the equation for the amplitude ψ_0 look the same as the equations for the amplitudes $\psi_{1,2}$, we introduced $\delta_0 = 0$. The Rabi frequencies of the laser fields obey the following propagation equations

$$(\partial_t + c\partial_z)\Omega_{j,l} = \frac{i}{2}g\psi_{e_j}\psi_l^*, \tag{43}$$

where the parameter g characterizes the strength of coupling of the light fields with the atoms.

Coupled and uncoupled states

Similarly to the M-type system, we introduce coupled (directly connected to the excited states via optical fields) and uncoupled (not coupled to the excited states) atomic states. The amplitudes of the two coupled states are $\psi_{C_j} = \Omega_j^{-1}\sum_{l=0}^{2}\Omega_{j,l}\psi_l$ where $\Omega_j = \sqrt{\sum_{l=0}^{2}|\Omega_{j,l}|^2}$. In addition, there is one uncoupled state

$$\psi_U = \frac{1}{N_0}\begin{vmatrix} \psi_0 & \psi_1 & \psi_2 \\ \Omega_{1,0}^* & \Omega_{1,1}^* & \Omega_{1,2}^* \\ \Omega_{2,0}^* & \Omega_{2,1}^* & \Omega_{2,2}^* \end{vmatrix} \equiv \sum_{l=0}^{2} A_l^*\psi_l, \tag{44}$$

Here, coefficients $A_0 = \frac{1}{N_0}(\Omega_{1,1}\Omega_{2,2} - \Omega_{1,2}\Omega_{2,1})$, $A_1 = \frac{1}{N_0}(\Omega_{1,2}\Omega_{2,0} - \Omega_{1,0}\Omega_{2,2})$, $A_2 = \frac{1}{N_0}(\Omega_{1,0}\Omega_{2,1} - \Omega_{1,1}\Omega_{2,0})$, and the normalization factor for the uncoupled state $N_0 = \left(|\Omega_{1,1}\Omega_{2,2} - \Omega_{1,2}\Omega_{2,1}|^2 + |\Omega_{1,2}\Omega_{2,0} - \Omega_{1,0}\Omega_{2,2}|^2 + |\Omega_{1,0}\Omega_{2,1} - \Omega_{1,1}\Omega_{2,0}|^2\right)^{1/2}$. Note, that $N_0^2 = \Omega_1^2\Omega_2^2 - \left(\sum_{l=0}^{2}\Omega_{2,l}^*\Omega_{1,l}\right)\left(\sum_{l=0}^{2}\Omega_{1,l}^*\Omega_{2,l}\right)$, and the coefficients A_l have the property $\sum_{l=0}^{2}A_l\Omega_{j,l} = 0$.

The initial atomic amplitudes then can be expressed as

$$\psi_l = A_l\psi_{\mathrm{U}} + \cdots \tag{45}$$

The equations (41), (42) for the atomic amplitudes in terms of coupled and uncoupled states take the form

$$i\partial_t\psi_{\mathrm{U}} = \Delta\psi_{\mathrm{U}} + \cdots\,, \tag{46}$$

$$i\partial_t\psi_{\mathrm{C}_j} = V_j\psi_{\mathrm{U}} - \frac{1}{2\Omega_j}\sum_m \psi_{e_m}\sum_{l=0}^{2}\Omega_{j,l}\Omega^*_{m,l}\,, \tag{47}$$

$$i\partial_t\psi_{e_j} = -\frac{i}{2}\Gamma\psi_{e_j} - \frac{1}{2}\Omega_j\psi_{\mathrm{C}_j}\,. \tag{48}$$

Here, the detuning $\Delta = \sum_{l=0}^{2} A_l(i\partial_t + \delta_l)A_l^*$, and coefficients $V_j = \Omega_j^{-1}\sum_{l=0}^{2} A_l(i\partial_t + \delta_l)\Omega_{j,l}$ describe the non-adiabatic coupling. The terms omitted in Eqs. (45) and (46) contain amplitudes ψ_{C_1} and ψ_{C_2}.

Adiabatic approximation

Let us consider a situation where the light fields are slowly changing and have large intensities. In this situation we can apply adiabatic approximation. Neglecting small amplitudes of the coupled states ψ_{C_1} and ψ_{C_2} in Eq. (47) leads to a system of equations

$$2\Omega_j V_j\psi_{\mathrm{U}} = \sum_m \psi_{e_m}\sum_{l=0}^{2}\Omega_{j,l}\Omega^*_{m,l}, \tag{49}$$

with the solution

$$\psi_{e_j} = 2W_j\psi_{\mathrm{U}}, \tag{50}$$

where

$$W_1 = \frac{1}{N_0^2}(\Omega_2^2\Omega_1 V_1 - \sum_{l=0}^{2}\Omega^*_{2,l}\Omega_{1,l}\Omega_2 V_2) = \frac{1}{N_0^2}\sum_{l=0}^{2} A_l\left(\Omega_2^2(i\partial_t+\delta_l)\Omega_{1,l} - \sum_{m=0}^{2}\Omega^*_{2,m}\Omega_{1,m}(i\partial_t+\delta_l)\Omega_{2,l}\right), \tag{51}$$

$$W_2 = \frac{1}{N_0^2}(\Omega_1^2\Omega_2 V_2 - \sum_{l=0}^{2}\Omega^*_{1,l}\Omega_{2,l}\Omega_1 V_1) = \frac{1}{N_0^2}\sum_{l=0}^{2} A_l\left(\Omega_1^2(i\partial_t+\delta_l)\Omega_{2,l} - \sum_{m=0}^{2}\Omega^*_{1,m}\Omega_{2,m}(i\partial_t+\delta_l)\Omega_{1,l}\right). \tag{52}$$

On the other hand, Eq. (48) relates ψ_{C_j} to ψ_{e_j} as $\psi_{\mathrm{C}_j} = -i(\Gamma/\Omega_j)\psi_{e_j}$. Neglecting the decay of adiabatons, Eq. (46) for the amplitude of the uncoupled state becomes $i\partial_t\psi_{\mathrm{U}} = \Delta\psi_{\mathrm{U}}$. Inserting Eq. (50) into Eq. (43) we get a set of equations

$$(\partial_t + c\partial_z)\Omega_{j,l} = igW_j A_l^*. \tag{53}$$

Equations (53) describe the adiabatic propagation of the fields. For the validity of the adiabatic approximation one should require that the population of the excited states be small compared to the population of the uncoupled state. According to Eq. (46) this leads to the adiabatic condition $|W_j| \ll 1$.

From Eq. (53) we obtain that the total Rabi frequencies Ω_j obey the equation

$$(\partial_t + c\partial_z)\Omega_j = 0, \tag{54}$$

meaning that Ω_j propagate without changing shape. In addition, for the coupling fields Rabi frequencies we have

$$(\partial_t + c\partial_z)\sum_{l=0}^{2}\Omega^*_{2,l}\Omega_{1,l} = 0. \tag{55}$$

Then, from both Eqs. (54), (55) follows that

$$(\partial_t + c\partial_z)N_0 = 0. \tag{56}$$

Thus the normalization factor N_0 also does not change shape during the propagation.

Matrix form of equations

Introducing the two-component spinors (columns) as $\hat{\Omega}_l = (\Omega_{1,l}, \Omega_{2,l})^{\mathsf{T}}$ we can write Eqs. (53) as

$$(c^{-1}\partial_t + \partial_z)\hat{\Omega}_l + A_l^*\hat{v}^{-1}\sum_{n=0}^{2}A_n(\partial_t - i\delta_n)\hat{\Omega}_n = 0, \tag{57}$$

where

$$\hat{v}^{-1} = \frac{g}{c}\frac{1}{N_0^2}\begin{pmatrix}\Omega_2^2 & -\sum_{m=0}^{2}\Omega^*_{2,m}\Omega_{1,m}\\ -\sum_{m=0}^{2}\Omega^*_{1,m}\Omega_{2,m} & \Omega_1^2\end{pmatrix}, \tag{58}$$

is the matrix of inverse group velocity[51] with the properties

$$\det \hat{v}^{-1} = \frac{g^2}{c^2 N_0^2}, \tag{59}$$

and

$$(\partial_t + c\partial_z)\hat{v}^{-1} = 0. \tag{60}$$

The eigenvalues of the matrix of inverse group velocity define the velocities of the propagating modes. These velocities increase with the amplitudes of the fields and are inversely proportional to atom-light coupling strength g. Also, from the equation (60) follows that the matrix $\hat{v}^{-1}$ does not change its z-dependent shape during the propagation.

Multiplying Eq. (57) by A_l and summing we get

$$\sum_{l=0}^{2} A_l (c^{-1}\partial_t + \partial_z)\hat{\Omega}_l + \hat{v}^{-1} \sum_{l=0}^{2} A_l (\partial_t - i\delta_l)\hat{\Omega}_l = 0. \tag{61}$$

Finally, using the matrix of inverse group velocity $\hat{v}^{-1}$ the adiabatic condition $|W_j| \ll 1$ in DT system can be written as

$$\frac{c}{g}\left| \hat{v}^{-1} \sum_{l=0}^{2} A_l (i\partial_t + \delta_l)\hat{\Omega}_l \right| \ll 1. \tag{62}$$

The condition should hold for each component of the column in vertical bars.

Adiabatons

Let us now consider the situation where there are no two-photon detunings, $\delta_l = 0$. We will search for a propagating solution in the form $\Omega_{j,l} = f_{j,l}\,(t - z/v_g)$. Then $\partial_z \Omega_{j,l} = -v_g^{-1}\partial_t \Omega_{j,l}$ and Eq. (57) becomes

$$v_g^{-1}\partial_t \hat{\Omega}_l = A_l^* \hat{v}^{-1} \sum_{n=0}^{2} A_n \partial_t \hat{\Omega}_n. \tag{63}$$

Multiplying this equation by A_l and summing over l we obtain

$$\hat{v}^{-1} \sum_{l=0}^{2} A_l \partial_t \hat{\Omega}_l = v_g^{-1} \sum_{l=0}^{2} A_l \partial_t \hat{\Omega}_l. \tag{64}$$

We see that in this case $\sum_{l=0}^{2} A_l \partial_t \hat{\Omega}_l$ should be an eigenvector of a matrix $\hat{v}^{-1}$, with v_g being the eigenvalue. Note, that since the adiabatic condition (62) contains inverse group velocity, the adiabaticity requirement for the solution with smaller value of v_g is stricter.

Let us write the eigenvector of the matrix $\hat{v}^{-1}$ corresponding to an eigenvalue v_g^{-1} as $(1, \xi)^T$. Since this eigenvector is equal to $\sum_{l=0}^{2} A_l \partial_t \hat{\Omega}_l$, we have $\sum_{l=0}^{2} A_l \partial_t \Omega_{2,l} = \xi \sum_{l=0}^{2} A_l \partial_t \Omega_{1,l}$. Then Eq. (63) can be written as

$$\partial_t \Omega_{1,l} = A_l^* \sum_{n=0}^{2} A_n \partial_t \Omega_{1,n}\,, \tag{65}$$

$$\partial_t \Omega_{2,l} = \xi A_l^* \sum_{n=0}^{2} A_n \partial_t \Omega_{1,n}, \tag{66}$$

or $\partial_t \Omega_{2,l} = \xi \partial_t \Omega_{1,l}$, with the solution $\Omega_{2,l}(t) - \xi \Omega_{1,l}(t) = \Omega_{2,l}(0) - \xi \Omega_{1,l}(0)$. Initially the pulses $\Omega_{1,0}$ and $\Omega_{2,0}$ are absent, thus $\Omega_{2,l}(t) = \xi \Omega_{1,l}(t)$. As a consequence of Eqs. (54), (55) the propagating solution obeys the equations

$$\Omega_j = \text{const}, \qquad \sum_{l=0}^{2} \Omega_{2,l}^* \Omega_{1,l} = \text{const}. \tag{67}$$

These equations ensure that the velocity v_g remains constant.

Let us consider the situation when $\Omega_{2,2}(0) = \Omega_{1,1}(0)$ and $\Omega_{2,1}(0) = \Omega_{1,2}(0)$. Then the eigenvalues are $v_g = \frac{c}{g}[\Omega_{1,1}(0) - \xi \Omega_{1,2}(0)]^2$ with $\xi = \pm 1$. From the equations it follows that $\Omega_{2,2} = \Omega_{1,1}$ and $\Omega_{2,1} = \Omega_{1,2}$ for

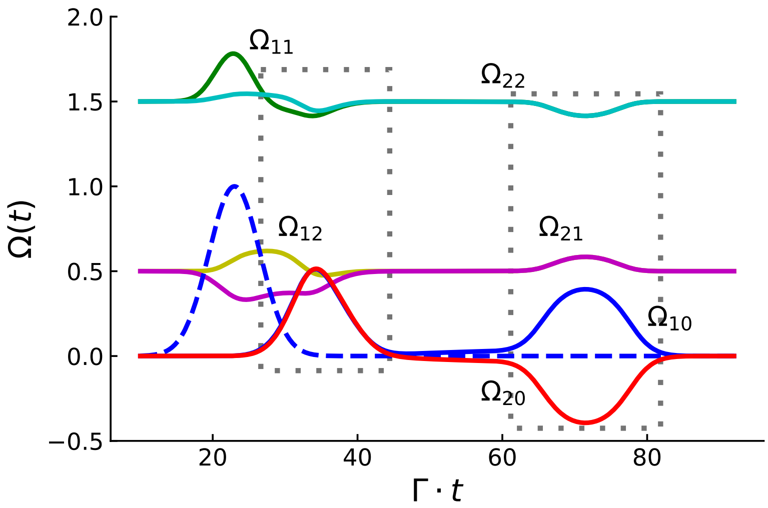

Fig. 3. Temporal dependence of pulse amplitudes in DT system. The dashed line corresponds to pulse envelope $\Omega_{1,0}$ at the input ($z = 0$), while the solid lines show pulse envelopes at the propagation distance $z = 50L_{\mathrm{abs}}$. Amplitude shown on the vertical scale is measured in Γ. There are two combinations of fields $\Omega_{j,l}$, indicated by two dotted rectangles, that propagate with different group velocities. The first combination, denoted by the right rectangle, has $\Omega_{2,0}(z,t) = -\Omega_{1,0}(z,t)$ and propagates with a smaller group velocity. The second combination, where $\Omega_{2,0}(z,t) = \Omega_{1,0}(z,t)$, propagates with a larger group velocity and is denoted by the left rectangle.

all times. The values of $\Omega_{1,1}$ and $\Omega_{1,2}$ can be found by solving the equations $\Omega_{1,2} - \xi\Omega_{1,1} = \Omega_{1,2}(0) - \xi\Omega_{1,1}(0)$, $\Omega_{1,0}^2 + \Omega_{1,1}^2 + \Omega_{1,2}^2 = \Omega_{1,1}^2(0) + \Omega_{1,2}^2(0)$.

Similarly to the previous cases, we used numerical calculations to demonstrate the obtained effects. At the beginning of the atomic medium two optical fields have Gaussian temporal shape: $\Omega_{1,0}(0,t) = A_1 \exp[-(t-t_1)^2/\tau_1^2]$, $\Omega_{2,0}(0,t) = A_2 \exp[-(t-t_2)^2/\tau_2^2]$, where $\tau_1 = \tau_2 = 5\Gamma^{-1}$, $t_1 = t_2 = 23\Gamma^{-1}$, $A_1 = \Gamma$, $A_2 = 0$; other fields are constant with amplitudes $\Omega_{1,1}(0,t) = \Omega_{2,2}(0,t) = 1.5\Gamma$ and $\Omega_{1,2}(0,t) = \Omega_{2,1}(0,t) = 0.5\Gamma$. Numerical results obtianed by solving Eqs. (53) are depicted in Fig. 3. It can be seen that there is adiabaton regime for the fields $\Omega_{j,l}$ after some propagation distance. There are two combinations of fields $\Omega_{j,l}$ propagating with different group velocities as indicated by two dotted rectangles in Fig. 3. The first combination, denoted by the right rectangle, is characterized by $\Omega_{2,0}(z,t) = -\Omega_{1,0}(z,t)$ and propagates with smaller group velocity. The second combination, denoted by the left rectangle, is characterized by $\Omega_{2,0}(z,t) = \Omega_{1,0}(z,t)$ and propagates with larger group velocity. Note, that the latter combination is not completely formed yet because it overlaps in time with the initial pulse $\Omega_{1,0}(0,t)$.

For the adiabatons to arise in the DT scheme the external fields should have large amplitudes and change slowly, so that the adiabatic condition given by Eq. (62) holds. The adiabatons should form whenever pulses of arbitrary shape are applied to optically thick five level media, assuming that amplitudes of the pulses are such that N_0 is not zero. The latter requirement follows from Eqs. (62) and (59).

Note that the practical limits of the adiabatic approximation are constrained by both intensity and duration of the optical pulses. The maximum intensities of the light pulses are limited by the presence of other atomic energy levels. Due to a.c. Stark effect induced by the fields, the atomic spectral shifts occur, and coupling to other atomic levels becomes possible. In order to avoid coupling to unwanted levels, Rabi frequencies should be small compared to the frequency differences between the atomic states involved. On the other hand, maximum pulse durations are limited by the decay rates of the adiabatons due to the non-adiabatic losses. We have presented the corresponding decay rates for Λ type systems in the Supplementary Information of this article. However, because of the relations complexity, we did not present the expressions for the non-adiabatic losses for the cases of more complex M-type and DT schemes.

Discussion, outlook and conclusions

To conclude, we have analyzed the propagation of optical pulses in multilevel M-type and double tripod (DT) atomic systems under the adiabatic approximation. Both schemes contain five non-degenerate atomic levels and exhibit an uncoupled (dark) state. We have derived equations for the adiabatic propagation of the light pulses for both setups, as represented by the Eqs. (29)–(32) and Eqs. (53), correspondingly. In the case of M-type atomic system the adiabatic regime is unstable as pulse group velocity depends on the amplitudes of the fields, making different part of the pulse propagate at different velocity. As a result, a region of the pulse with large steepness appears and the adiabatic approximation becomes not valid after some distance. In contrast, in the DT system a long range adiabatic propagation of light pulses is possible and is characterized by two different configurations of fields propagating with invariant shape. Here, the optical adiabaton arises as a result of a transformation of six coupled optical fields into a robust shape-preserving combination. The difference between M-type and DT systems demonstrates that adiabaton formation is not commonly supported even for comparable energy-level structures in EIT-enabled multilevel setups (Fig. 1). Rather, it implies that the adiabatic propagation of light pulses is quite sensitive to optical fields arrangement and interaction configuration.

It should be noted that we have omitted decoherence effects in our study to focus on the ideal adiabatic scenario. Decoherence inherently degrades the lossless, shape-preserving propagation of adiabatons leading to their eventual decay. In practice, the coherence loss can be mitigated by the techniques such as optical pumping or dynamical decoupling. Similarly, we excluded all forms of inhomogeneous broadening, including Doppler broadening, from the theoretical model. Doppler broadening arises from the thermal motion of atoms, shifting resonance frequencies and broadening spectral lines, which induces a spread of group velocities that can distort pulse shapes. The resulting nonuniform coupling between the probe and control fields undermines the ground-state coherence required for shape-invariant propagation. However, the experimental techniques employed for cold-atom systems can effectively suppress these effects making the idealized adiabatic regime readily attainable.

The DT configuration for the adiabaton propagation presented here can be realized experimentally similarly to that used in[51] where an ensemble of laser-cooled Rb atoms loaded into magneto-optical trap was explored. Specifically, the atomic levels $|5S_{1/2}, F=1, m=0\rangle$, $|5S_{1/2}, F=2, m=0\rangle$ and $|5S_{1/2}, F=2, m=2\rangle$ can be used as the ground states $|0\rangle$, $|1\rangle$ and $|2\rangle$, whereas the atomic levels $|5P_{1/2}, F=2, m=1\rangle$ and $|5P_{3/2}, F=2, m=1\rangle$ as the excited states $|e_1\rangle$ and $|e_2\rangle$, respectively. By choosing the appropriate intensities of the coupling laser fields, the results of the theoretical model presented in Fig. 3 can be verified experimentally.

While the current study only addresses the temporal dynamics of one-dimensional pulses, there are plans to extend this analysis to pulses of more complex shapes, like those having transverse intensity structure or carrying orbital angular momentum. That would require the use of paraxial propagation equations describing the transverse evolution of the beam, allowing to investigate the impact of additional degrees of freedom on adiabaton formation.

Data availability

The datasets used and/or analyzed during the current study are available from the corresponding author on reasonable request.

Received: 24 February 2025; Accepted: 5 June 2025
Published online: 12 July 2025

References

1. Li, G.-X., Li, F.-L. & Zhu, S.-Y. Quantum interference between decay channels of a three-level atom in a multilayer dielectric medium. *Phys. Rev. A* **64**, 013819. https://doi.org/10.1103/PhysRevA.64.013819 (2001).
2. Fleischhauer, M., Imamoglu, A. & Marangos, J. P. Electromagnetically induced transparency: Optics in coherent media. *Rev. Mod. Phys.* **77**, 633–673. https://doi.org/10.1103/RevModPhys.77.633 (2005).
3. Kalashnikov, D. A. et al. Quantum interference in the presence of a resonant medium. *Sci. Reports* **7**, 11444. https://doi.org/10.1038/s41598-017-11694-z (2017).
4. Harris, S. E. Electromagnetically induced transparency. *Phys. Today* **50**, 36–42. https://doi.org/10.1063/1.881806 (1997).
5. Wu, Y. & Yang, X. Electromagnetically induced transparency in V-, Λ-, and cascade-type schemes beyond steady-state analysis. *Phys. Rev. A* **71**, 053806. https://doi.org/10.1103/PhysRevA.71.053806 (2005).
6. Hamedi, H. R., Ruseckas, J. & Juzeliunas, G. Electromagnetically induced transparency and nonlinear pulse propagation in a combined tripod and Λ atom-light coupling scheme. *J. Phys. B: Atomic, Mol. Opt. Phys.* **50**, 185401. https://doi.org/10.1088/1361-6455/aa84f6 (2017).
7. Arimondo, E. V coherent population trapping in laser spectroscopy. *Progress Opt.* **35**, 257–354. https://doi.org/10.1016/S0079-6638(08)70531-6 (1996).
8. Hau, L. V., Harris, S. E., Dutton, Z. & Behroozi, C. H. Light speed reduction to 17 metres per second in an ultracold atomic gas. *Nature* **397**, 594–598. https://doi.org/10.1038/17561 (1999).
9. Wang, H., Goorskey, D. & Xiao, M. Enhanced Kerr nonlinearity via atomic coherence in a three-level atomic system. *Phys. Rev. Lett.* **87**, 073601. https://doi.org/10.1103/PhysRevLett.87.073601 (2001).
10. Lukin, M. D. Colloquium: Trapping and manipulating photon states in atomic ensembles. *Rev. Mod. Phys.* **75**, 457–472. https://doi.org/10.1103/RevModPhys.75.457 (2003).
11. Niu, Y. & Gong, S. Enhancing Kerr nonlinearity via spontaneously generated coherence. *Phys. Rev. A* **73**, 053811. https://doi.org/10.1103/PhysRevA.73.053811 (2006).
12. Hamedi, H. R. & Juzeliunas, G. Phase-sensitive Kerr nonlinearity for closed-loop quantum systems. *Phys. Rev. A* **91**, 053823. https://doi.org/10.1103/PhysRevA.91.053823 (2015).
13. Paspalakis, E. & Kis, Z. Enhanced nonlinear generation in a three-level medium with spatially dependent coherence. *Opti. Lett.* **27**, 1836–1838. https://doi.org/10.1364/OL.27.001836 (2002).
14. Paspalakis, E., Kylstra, N. J. & Knight, P. L. Propagation and nonlinear generation dynamics in a coherently prepared four-level system. *Phys. Rev. A* **65**, 053808. https://doi.org/10.1103/PhysRevA.65.053808 (2002).
15. Kis, Z. & Paspalakis, E. Enhancing nonlinear frequency conversion using spatially dependent coherence. *Phys. Rev. A* **68**, 043817. https://doi.org/10.1103/PhysRevA.68.043817 (2003).
16. Wu, Y. & Deng, L. Ultraslow optical solitons in a cold four-state medium. *Phys. Rev. Lett.* **93**, 143904. https://doi.org/10.1103/PhysRevLett.93.143904 (2004).
17. Wu, Y. & Deng, L. Ultraslow bright and dark optical solitons in a cold three-state medium. *Opt. Lett.* **29**, 2064–2066. https://doi.org/10.1364/OL.29.002064 (2004).
18. Li, J.-H., Lu, X.-Y., Luo, J.-M. & Huang, Q.-J. Optical bistability and multistability via atomic coherence in an N-type atomic medium. *Phys. Rev. A* **74**, 035801. https://doi.org/10.1103/PhysRevA.74.035801 (2006).
19. Clader, B. D. & Eberly, J. H. Two-pulse propagation in media with quantum-mixed ground states. *Phys. Rev. A* **76**, 053812. https://doi.org/10.1103/PhysRevA.76.053812 (2007).
20. Wu, Y. & Yang, X. Four-wave mixing in molecular magnets via electromagnetically induced transparency. *Phys. Rev. B* **76**, 054425. https://doi.org/10.1103/PhysRevB.76.054425 (2007).
21. Chen, Y., Bai, Z. & Huang, G. Ultraslow optical solitons and their storage and retrieval in an ultracold ladder-type atomic system. *Phys. Rev. A* **89**, 023835. https://doi.org/10.1103/PhysRevA.89.023835 (2014).
22. Dong, H. M., Hien, N. T. T., Bang, N. H. & Doai, L. V. Dynamics of twin pulse propagation and dual-optical switching in a $\Lambda + \Xi$ atomic medium. *Chaos, Solitons & Fractals* **178**, 114304. https://doi.org/10.1016/j.chaos.2023.114304 (2024).

23. Zhang, Z. et al. Observation of edge solitons in photonic graphene. *Nat. Commun.* **11**, 1902. https://doi.org/10.1038/s41467-020-15635-9 (2020).
24. Li, K. et al. Direct generation of time-energy-entangled W triphotons in atomic vapor. *Sci. Adv.* **10**, 3199. https://doi.org/10.1126/sciadv.ado3199 (2024).
25. Ali, S., Idrees, M., Bacha, B. A., Ullah, A. & Haneef, M. Efficient two-dimensional atom localization in a five-level conductive chiral atomic medium via birefringence beam absorption spectrum. *Commun. Theoret. Phys.* **73**, 015102. https://doi.org/10.1088/1572-9494/abc46c (2020).
26. Din, R. U., He, Q., Bacha, B. A., Ahmad, I. & Ge, G.-Q. Unusual refraction and Fizeau effect for a linearly polarized pulse in rotary chiral media. *J. Opt. Soc. Am. B* **35**, 1817–1824. https://doi.org/10.1364/JOSAB.35.001817 (2018).
27. Ghafoor, F., Bacha, B. A. & Khan, S. Inverse Doppler shift and control field as coherence generators for the stability in superluminal light. *Phys. Rev. A* **91**, 053807. https://doi.org/10.1103/PhysRevA.91.053807 (2015).
28. Meng, C., Shui, T. & Yang, W.-X. Coherent transfer of optical vortices via backward four-wave mixing in a double-Λ atomic system. *Phys. Rev. A* **107**, 053712. https://doi.org/10.1103/PhysRevA.107.053712 (2023).
29. Deng, X., Shui, T. & Yang, W.-X. Inelastic two-wave mixing induced high-efficiency transfer of optical vortices. *Opt. Express* **32**, 16611–16628. https://doi.org/10.1364/OE.516310 (2024).
30. Huang, C. et al. Electromagnetically induced transparency cooling of high-nuclear-spin ions. *Phys. Rev. Lett.* **133**, 113204. https://doi.org/10.1103/PhysRevLett.133.113204 (2024).
31. Chu, K.-I. et al. Slow and stored light via electromagnetically induced transparency using a Λ-type superconducting artificial atom. *Phys. Rev. Res.* **7**, L012015. https://doi.org/10.1103/PhysRevResearch.7.L012015 (2025).
32. Zhang, T.-H., Wang, W.-M., Li, Y.-T. & Zhang, J. Electromagnetically induced transparency in the strongly relativistic regime. *Phys. Rev. Lett.* **132**, 065105. https://doi.org/10.1103/PhysRevLett.132.065105 (2024).
33. Hoang Minh, D., Luongthiyen, N., Dinh Xuan, K. & Nguyen Huy, B. Controllable ultraslow optical solitons in a degenerated two-level atomic medium under EIT assisted by a magnetic field. *Sci. Reports* **10**, 15298. https://doi.org/10.1038/s41598-020-72256-4 (2020).
34. Zhu, J. & Huang, G. Quantum squeezing of slow-light dark solitons via electromagnetically induced transparency. *Phys. Rev. A* **105**, 033515. https://doi.org/10.1103/PhysRevA.105.033515 (2022).
35. Zhang, H., Li, Z., Wang, Y., Hang, C. & Wu, G. Observation of ultraslow optical solitons and vortex solitons in a room-temperature atomic gas via electromagnetically induced transparency. *Chaos, Solitons & Fractals* **192**, 116058. https://doi.org/10.1016/j.chaos.2025.116058 (2025).
36. Grobe, R., Hioe, F. T. & Eberly, J. H. Formation of shape-preserving pulses in a nonlinear adiabatically integrable system. *Phys. Rev. Lett.* **73**, 3183–3186. https://doi.org/10.1103/PhysRevLett.73.3183 (1994).
37. Fleischhauer, M. & Manka, A. S. Propagation of laser pulses and coherent population transfer in dissipative three-level systems: An adiabatic dressed-state picture. *Phys. Rev. A* **54**, 794–803. https://doi.org/10.1103/PhysRevA.54.794 (1996).
38. Kasapi, A., Jain, M., Yin, G. Y. & Harris, S. E. Electromagnetically induced transparency: Propagation dynamics. *Phys. Rev. Lett.* **74**, 2447–2450. https://doi.org/10.1103/PhysRevLett.74.2447 (1995).
39. Cerboneschi, E. & Arimondo, E. Propagation and amplitude correlation of pairs of intense pulses interacting with a double-Λ system. *Phys. Rev. A* **54**, 5400–5409. https://doi.org/10.1103/PhysRevA.54.5400 (1996).
40. Buffa, R., Cavalieri, S. & Tognetti, M. V. Coherent control of temporal pulse shaping by electromagnetically induced transparency. *Phys. Rev. A* **69**, 033815. https://doi.org/10.1103/PhysRevA.69.033815 (2004).
41. Arkhipkin, V. G. & Timofeev, I. V. Temporal shape manipulation of intense light pulses by coherent population trapping. *Phys. Rev. A* **73**, 025803. https://doi.org/10.1103/PhysRevA.73.025803 (2006).
42. Shakhmuratov, R. N. & Odeurs, J. Two types of adiabatons in electromagnetically induced transparency. *Phys. Rev. A* **74**, 043807. https://doi.org/10.1103/PhysRevA.74.043807 (2006).
43. Mazets, I. E. Adiabatic pulse propagation in coherent atomic media with the tripod level configuration. *Phys. Rev. A* **71**, 023806. https://doi.org/10.1103/PhysRevA.71.023806 (2005).
44. Hioe, F. T. Adiabatic shape preservation and solitary waves in a five-level atomic medium. *Phys. Rev. A* **78**, 063807. https://doi.org/10.1103/PhysRevA.78.063807 (2008).
45. Li, L., Guo, H., Xiao, F., Peng, X. & Chen, X. Control of light in an M-type five-level atomic system. *J. Opt. Soc. Am. B* **22**, 1309–1313. https://doi.org/10.1364/JOSAB.22.001309 (2005).
46. Gu, Y., Wang, L., Wang, K., Yang, C. & Gong, Q. Coherent population trapping and electromagnetically induced transparency in a five-level M-type atom. *J. Phys. B: Atom., Mol. Opt. Phys.* **39**, 463–470. https://doi.org/10.1088/0953-4075/39/3/004 (2006).
47. Unanyan, R. G. et al. Spinor slow-light and Dirac particles with variable mass. *Phys. Rev. Lett.* **105**, 173603. https://doi.org/10.1103/PhysRevLett.105.173603 (2010).
48. Ruseckas, J. et al. Photonic-band-gap properties for two-component slow light. *Phys. Rev. A* **83**, 063811. https://doi.org/10.1103/PhysRevA.83.063811 (2011).
49. Ruseckas, J., Kudriaov, V., Yu, I. A. & Juzeliunas, G. Transfer of orbital angular momentum of light using two-component slow light. *Phys. Rev. A* **87**, 053840. https://doi.org/10.1103/PhysRevA.87.053840 (2013).
50. Bao, Q.-Q. et al. Coherent generation and dynamic manipulation of double stationary light pulses in a five-level double-tripod system of cold atoms. *Phys. Rev. A* **84**, 063812. https://doi.org/10.1103/PhysRevA.84.063812 (2011).
51. Lee, M.-J. et al. Experimental demonstration of spinor slow light. *Nat. Commun.* **5**, 5542. https://doi.org/10.1038/ncomms6542 (2014).
52. Eberly, J. H. Transmission of dressed fields in three-level media. *Quantum and Semiclassical Opt.* **7**, 373–384. https://doi.org/10.1088/1355-5111/7/3/013 (1995).
53. Chuang, Y.-L., Lee, R.-K. & Yu, I. A. Optical-density-enhanced squeezed-light generation without optical cavities. *Phys. Rev. A* **96**, 053818. https://doi.org/10.1103/PhysRevA.96.053818 (2017).
54. DeMartini, F., Townes, C. H., Gustafson, T. K. & Kelley, P. L. Self-steepening of light pulses. *Phys. Rev.* **164**, 312–323. https://doi.org/10.1103/PhysRev.164.312 (1967).
55. Suydam, B. R. *Self-Steepening of Optical Pulses* 295-295–317 (Springer, New York, 1989).

Acknowledgements
This project has received funding from the Research Council of Lithuania (LMTLT), agreement No. S-ITP-24-6.

Author contributions
J.R. originated the idea and developed the theoretical model. J.R. and V.K. performed analysis, numerical study, described results and wrote the manuscript. H.R.H. wrote parts of the manuscript and compiled the final version. All authors contributed to discussion and interpretation, editing and reviewing.

Declarations

Competing interests
The authors declare no conflict of interest.

Additional information
Supplementary Information The online version of this article (https://doi.org/10.1038/s41598-025-05950-w) contains supplementary material, which is available to authorized users.

Correspondence and requests for materials should be addressed to H.R.H.

Reprints and permissions information is available at www.nature.com/reprints.

Publisher's note Springer Nature remains neutral with regard to jurisdictional claims in published maps and institutional affiliations.